ECS Transactions, 58 (1) 293-299 (2013)
10.1149/05801.0293ecst ©The Electrochemical Society

Neutron Imaging Of Water Transport In Polymer-Electrolyte Membranes And Membrane-Electrode Assemblies

D.S. Hussey[a], D. Spernjak[b], G. Wu[b], D.L. Jacobson[a],
D. Liu[c], B. Khaykovich[c], M.V. Gubarev[d],
J. Fairweather[b], R. Mukundan[b], R. Lujan[b], P. Zelenay[b], and R.L. Borup[b]

[a] National Institute of Standards and Technology, Gaithersburg, MD 20899, USA
[b] Los Alamos National Laboratory, Los Alamos, NM 87545, USA
[c] Massachusetts Institute of Technology, Cambridge, MA0 2139, USA
[d] Marshall Space Flight Center, NASA, Huntsville, AL 35812, USA

Neutron imaging was been widely used to study the water distribution in proton exchange membrane fuel cell flow fields and gas diffusion layer. However, due to the limitation of spatial resolution, there has been little focus on the water transport process in the membrane and catalyst layer. Here we report on measurements made on thick membranes under saturation gradients which show no "jump condition" and on thick cathode catalyst layers to understand the water transport issues in a non-precious metal catalyst. Finally, we speculate on the possibility of obtaining neutron images with ~1 µm spatial resolution.

Introduction

A typical feature of water-transport models of proton exchange membrane fuel cells (PEFMCs) is a jump condition that accounts for Schroeder's paradox, which is the observation that Nafion[1] undergoes a step change in water content when the inlet gas relative humidity (RH) changes from 100 % to oversaturated (i.e. liquid water). The water content of the membrane is reported as moles of water per moles of sulfonic acid sites (λ). With 100 % RH, $\lambda_{100} \sim 13$, in oversaturated conditions $\lambda_s \sim 20$, exact values depend on temperature, membrane history and composition. Under many operating conditions, there will be a liquid water layer (or, distribution) in the cathode catalyst, thus the cathode-side of the membrane will have $\lambda \sim 20$. The anode inlet stream is typically under-saturated so that $\lambda < \lambda_{100}$. In the jump condition approach, Schroeder's paradox is incorporated by having $\lambda \sim \lambda_s$ from the cathode until the water activity is less than 1, where it rapidly drops to $\lambda < \lambda_{100}$. Under this assumption, there would be a very large pressure gradient at the jump location due to the drop in water content, and this is not physical. Indeed, other groups have studied the through-plane water content of Nafion under saturation gradients and have seen a smooth gradient in water content.(1) Having recently established the process for obtaining the accurate water content in membranes (2, 3), we performed measurements using neutron imaging to confirm the gradient results

[1] Certain trade names and company products are mentioned in the text or identified in an illustration in order to adequately specify the experimental procedure and equipment used. In no case does such identification imply recommendation or endorsement by the National Institute of Standards and Technology, nor does it imply that the products are necessarily the best available for the purpose.

with a non-destructive probe as opposed to x-rays which have been shown to alter the material properties under x-ray exposure (4).

Current estimates assign 40 % of the cost of automotive PEMFC engines at high volume production to the platinum used in the catalyst layer. Many efforts are underway to reduce the amount of platinum in the cathode catalyst layer using core shell particles, alloys, and thin film structures. As well, research is ongoing to develop oxygen reduction reaction catalysts that use only non-precious metals. One of the more promising candidates for these is a N-Fe-C catalyst derived from a polyaniline precursor (PANI) (5). This catalyst shows catalytic activity that is half that of Pt and is stable enough to be used in a membrane electrode assembly. However, this PANI catalyst layer is thick, of order 100 µm, and mass transport through this thick layer will likely impact the performance of a PEMFC with such a cathode. In order to understand how the PANI catalyst properties impacted the performance, we compared a PANI catalyst to a Pt-black with a similar thickness.

Neutron imaging has been a valuable tool for studying *in operando* a variety of water transport processes in PEMFCs. The reason for this is a result of neutrons having a high transmission through the common materials of fuel cell construction (carbon, aluminum, stainless steel) yet still having a very high sensitivity to water. A review of the method of neutron imaging and the transport processes studied in flow fields can be found by Trabold, et al,(6) and a review of transport in the gas diffusion media by Hussey and Jacobson.(7) We briefly review two important considerations for neutron imaging, the physics of neutron detection and counting statistics.

The obtainable spatial resolution in neutron images is limited by the physics of neutron detection. Because neutrons are neutral particles, neutron detection occurs through a multiple step process. The neutron is first captured by a nucleus with a large absorption cross-section; typical isotopes include 3-He, 6-Li, 10-B, and 158-Gd. The excited nucleus then decays through emission of an energetic charged particle. In the case of scintillators, the particle moves through the matrix emitting light as energy is exchanged with the scintillator. In microchannel plates (MCPs), the particles move through the glass walls and strip electrons from the inner surface.(8) In both cases, the range of the charged particle ranges from 5 µm to 30 µm, and since the particle is emitted in all directions, the resulting resolution is about twice the range. Over the course of several years, the resolution of neutron imaging improved from about 250 µm to ~10 µm, reaching this fundamental physical limit due to the charged particle range.

Neutron imaging is conventionally a pinhole camera; the geometry of the setup must be controlled to reach the resolution of the detector. Specifically, the geometric unsharpness, $\lambda_g = z\ d / L$, where z is the separation between the sample and detector, d is the dimension of the beam defining aperture, and L is the distance between the aperture and the detector. For typical high resolution imaging of PEMFCs, the active area is about 3 cm from the detector surface, thus to have λ_g = 5 µm, d/L = 1/6000. The neutron fluence rate (neutrons per area per time) at the sample varies as $(d/L)^2$; thus in order to achieve high spatial resolution, one sacrifices neutron intensity. A typical neutron fluence rate is ~10^6 cm^{-2} s^{-1}, so in a 10 µm pixel one neutron is incident per second on average. Thus, in order to have a ~1 % relative uncertainty measurement of the neutron transmission of the open beam, the image acquisition time is about 20 min. In PEFMC

imaging, higher time resolution of the water content along the PEMFC through-plane direction can be achieved if one averages along the in-plane direction.

Experimental

All imaging was performed at the neutron imaging facility located at the NIST Center for Neutron Research.(9) Images were acquired with an MCP detector with cross-strip readout that has a nominal spatial resolution of 13 µm defined as the point at which the modulation transfer function reaches 10 %. The beam collimation settings used a slit aperture, with the long dimension (10 mm tall) of the slit aligned with the in-plane direction of the fuel cell and the short dimension (1 mm wide) aligned with the through-plane direction, and the distance from the aperture to the detector was about 6 m. The test section was allowed to equilibrate at a given condition for at least 15 minutes, and images were acquired for at least 20 minutes after equilibration.

The test sections were specifically designed for high resolution neutron imaging, and details of the design are discussed elsewhere.(2, 10) The end plates and flowfields were machined in aluminum and then gold coated to prevent corrosion. The active area of the test sections was approximately 2 cm by 1 cm, with the neutron beam passing through the 1 cm width. For the membrane saturation gradient measurements, metal foam flow fields were used (instead of the usual channels and lands) to support the membrane and to minimize other contributions to water transport. In order to resolve water gradients within the membrane, ~300 µm thick Nafion membranes produced by Ion Power were used. The humidity of the inlet and outlet gas streams was measured by a Viasala humidity sensor and a high gas flow rate of 0.8 slpm was used to approximately generate a uniform humidity along the length of the membrane. For imaging experiment involving the thick catalyst layers, the catalysts were painted on to cloth gas diffusion layers. The PANI catalyst ranged in thickness from 70 µm to 80 µm and the Pt-black catalyst thickness ranged from 50 µm to 55 µm, as determined by post mortem x-ray tomography analysis. The cells were operated at 80 °C at 50 % and 100 % inlet RH, using hydrogen and air; the cloth GDLs necessitated a high back pressure of 206 kPa. Images were acquired at three current densities: open circuit voltage (OCV), 0.2 A/cm^2 and 0.4 A/cm^2.

Results

Shown in Figure 1 is the summary of all the hydration gradient data taken. The raw neutron radiographs were processed according to the procedure detailed in Hussey, et al.(2) Three assumptions were that the residual λ in the dry state was λ_{dry}=2.5; the membrane was in a free swelling state so that $\chi = 0$; for λ=22, the maximum swelling was 12.5 %. As can be seen from the data taken with the same saturation on either side of the membrane (four values of 50 %, 75 %, 100 %, 175 %), the obtained λ are in agreement with *ex situ* measurements. The observed water content at 100 % RH is $\lambda = 11$. Under the a hydration gradient of 0 % RH and 100 % RH, the maximum value of the water content on the saturated side is strongly reduced. This trend is also observed for the 0 % RH and 175 % RH condition, where the water content on the over-saturated side, while higher than that observed at 100 %, is still below that observed in liquid saturation. At 100 % RH and 175 % RH shows that the gradient in the water content depends on the history, where the desorption step shows both a higher average water content and a stronger gradient than in the sorption step. It should be emphasized that these data are

after the water content had 30 minutes to evolve. These data are in qualitative agreement with that of Hwang, et al,(1) and do not support a jump condition model to the water content in the membrane.

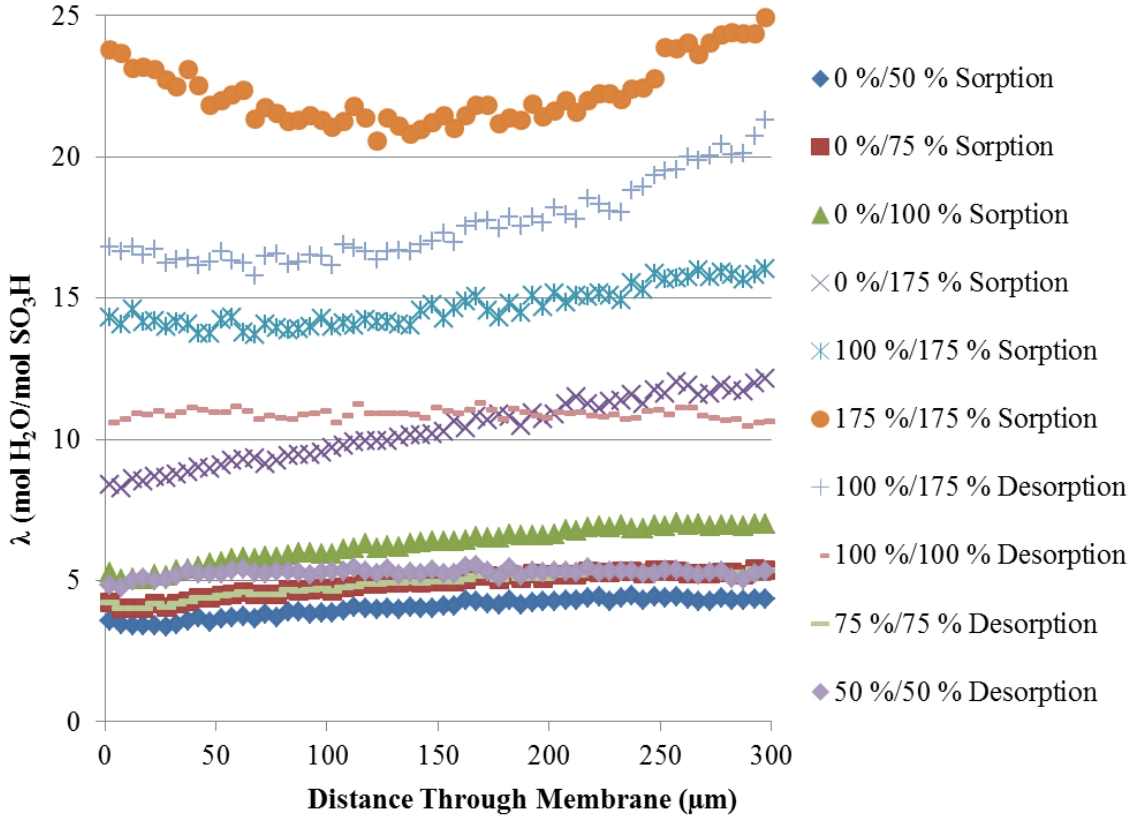

Figure 1. Summary of all hydration gradient data at 80 °C. The data were taken after at least 30 minutes equilibration time at the given saturation condition, followed by image acquisition over another 30 minutes. Images were acquired with 2 minute exposure times to track any time variation in the water content that was measurable with the neutron counting statistics. The membrane was fully supported, but assumed to be in a free-swelling state and the analysis of such a system is given in Hussey et al.(2)

Shown in Figure 2 and Figure 3 is the measured through-plane water content under the lands for the test sections with PANI and Pt-Black catalyst layers, respectively. (Under the channel data was difficult to compare due to the use of cloth GDLs.) In all cases the PANI cell has significantly more water entrained in the sandwich which is a clear indication that this excess water content will contribute to mass transport losses. Since the Pt-black catalyst is nominally the same thickness and has significantly less water, the observed mass transport losses in the PANI cell are not primarily due to the thickness of the catalyst. An important feature of the data comes from comparing the water profiles of the two cells at OCV. In the case of Pt-black, there is a slight difference between 50 % RH and 100 % RH at OCV, and as well, the water content is a maximum in the center of the membrane, and decays rapidly in the cathode catalyst layer. This is somewhat expected, as these profiles are not corrected for any blurring due to the detector resolution. In contrast, the PANI cell shows a small peak at the catalyst / membrane interface, and the water content is about twice that of the Pt-black. This indicates that there is either poor contact with the membrane and water is pooling in these voids or that the interface (and hence the catalyst layer) is slightly hygroscopic, as both the 50 % RH and 100 % RH OCV water contents are similar at this interface.

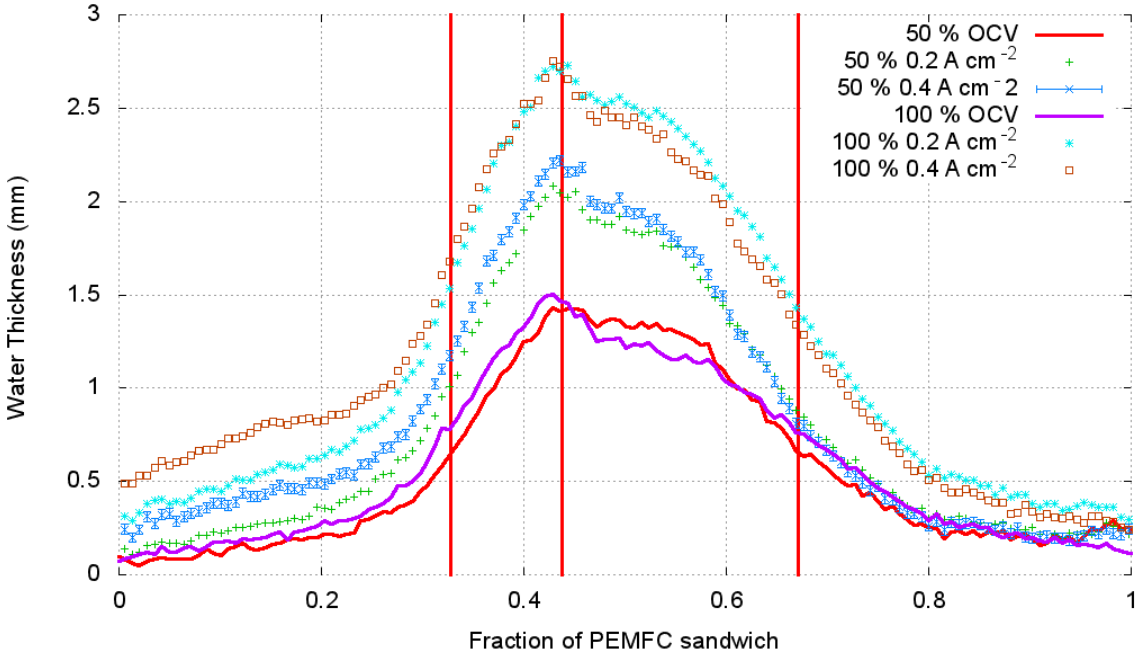

Figure 2. Through-plane water content of the non-precious metal catalyst at 206 kPa at the test current densities. The leftmost vertical red line is the cathode catalyst/GDL interface, the middle line is the cathode catalyst/membrane interface, and the rightmost line is the membrane/anode GDL interface.

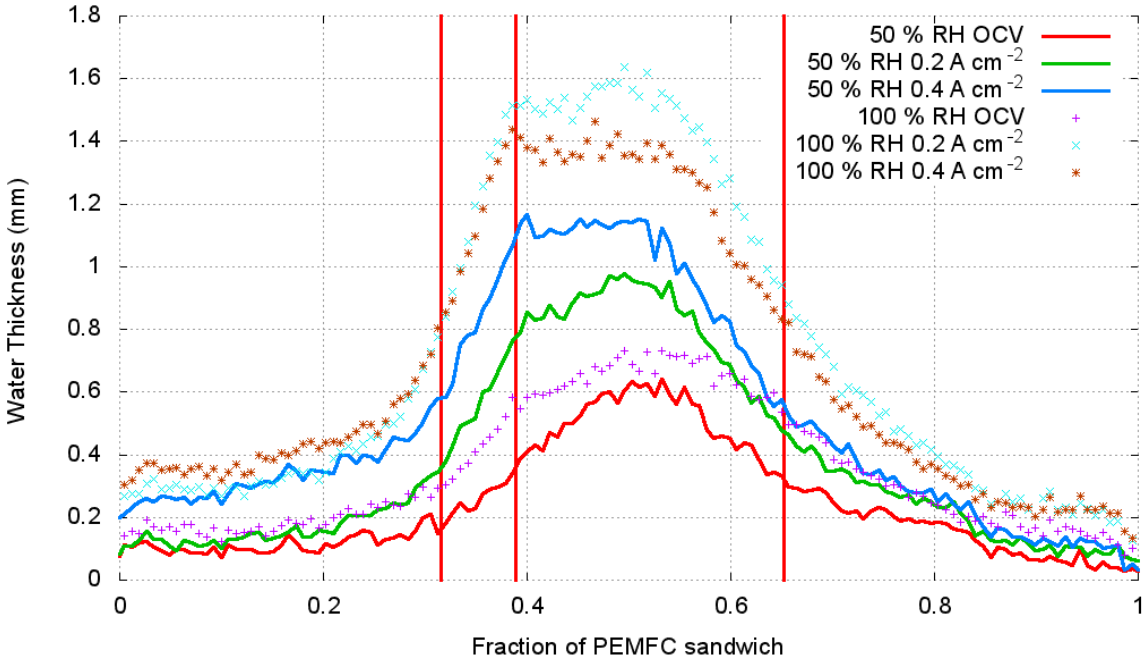

Figure 3. Through-plane water content of the Pt-black catalyst at 206 kPa at the test current densities. The leftmost vertical red line is the cathode catalyst/GDL interface, the middle line is the cathode catalyst/membrane interface, and the rightmost line is the membrane/anode GDL interface.

These observations point to several engineering solutions that can improve the performance of a fuel cell with a PANI catalyst. The first is to move from catalyst coated cloth GDLs to catalyst coated membranes to ensure that there are no voids between the membrane and the catalyst layer. As well, using paper GDLs will not intrude into the channels and will reduce the pressure differential during operation. Lastly, one can take inspiration from the work to improve the performance 3M's nano-structured thin film catalyst which also suffers from cathode catalyst flooding.(11) It has been noted that by using a hydrophilic GDL on the anode, one increases the back-diffusion through the membrane and thus wicks water away from the cathode catalyst through the anode. These experiments have been recently performed and results will be forthcoming.

Outlook

While the model systems described above yield insight into the water transport processes in membranes and catalyst layers, neutron imaging would be able to make a better contribution to the further development of PEMFCs if the technique can resolve the features in commercially competitive membranes and common catalyst layers. As mentioned in the Introduction, there are two hurdles to obtaining higher spatial resolution neutron images: the range of the charged particle from the neutron capture reaction and the inherently low neutron counts due to pinhole optics. There are currently two proposals to reach a spatial resolution of 1 µm that would enable studying the membrane electrode assembly in more detail. The first is to scan the fuel cell with an assembly of narrow slits (a grating) that are well-resolved from one another and thereby obtain a high resolution image in one direction. The limitation of this method is that it is time consuming due to scanning and low neutron counts due to the narrow slit with an image requiring at least 12 h to acquire. This long acquisition will require fuel cells to be very stable at a given condition. The technique was demonstrated using 10 µm wide slits, to improve on this, new grating fabrication techniques are required, and this has proved challenging due to the need for thick deposits of Gd, the strongest neutron absorber.

The second proposal is a completely new method of acquiring neutron images and uses a reflective neutron lens developed by NASA and has recently been demonstrated at NIST.(12) In this case, one no longer uses pinhole optics as the basis for image formation; instead the lens forms a real image at the detector in a similar fashion to a visible light microscope. Two primary advantages of this approach are: one does not need to collimate the beam to obtain resolution, thereby increasing the neutron intensity by a factor of 100 and by using different focal lengths one can magnify the image, with a 10x objective being practicable an ultimate resolution of 1 µm can be achieved. Since the intensity has also been increased by ~100, the time to acquire an image with 1 µm resolution would be similar to the time for a 10 µm resolution image. The fabrication method to achieve this 1 µm resolution is still being developed, and it is thought that within 3 to 5 years will have matured to the point where a neutron microscope can be built.

Conclusions

We have performed neutron imaging experiments to measure the water content in thick membranes under hydration gradients and in thick catalyst layers. The results confirm that no jump-condition is observed in the membrane under a hydration gradient, but

rather that the water content is smooth. The non-precious metal catalyst based on Fe from a polyaniline precursor were observed to be very hydrophilic, perhaps hygroscopic, and several engineering avenues for improving the water transport in these novel catalysts were identified. Work proceeds to improve the spatial resolution of neutron imaging, with a neutron microscope being the most promising for fuel cell development.

Acknowledgments

The authors would like to thank Dr. Stephen Grot of Ion Power for generating the extra-thick Nafion membranes and Mr. Eli Baltic of NIST for assistance with performing the neutron imaging experiments. We thank Nuvera Fuel Cells for providing the metal-foam flow fields used in the sorption measurements. The Los Alamos team gratefully acknowledges the support of the technology development manager Nancy Garland, and funding from the US Department of Energy, the Office of Energy Efficiency and Renewable Energy, Office of Fuel Cell Technologies. D. S. Hussey and D. L. Jacobson acknowledge support from the U.S. Department of Commerce, the NIST Ionizing Radiation Division, the Director's office of NIST, the NIST Center for Neutron Research, and the Department of Energy interagency Agreement No. DE_AI01-01EE50660.

References

1. G. S. Hwang, D. Y. Parkinson, A. Kusoglu, A. A. MacDowell and A. Z. Weber, *Acs Macro Letters*, **2**, 288 (2013).
2. D. S. Hussey, D. Spernjak, A. Z. Weber, R. Mukundan, J. Fairweather, E. L. Brosha, J. Davey, J. S. Spendelow, D. L. Jacobson and R. L. Borup, *Journal of Applied Physics*, **112** (2012).
3. D. Spernjak, P. P. Mukherjee, R. Mukundan, J. Davey, D. S. Hussey, D. Jacobson and R. L. Borup, *ECS Transactions*, **33**, 1451 (2010).
4. J. Roth, J. Eller and F. N. Buchi, *Journal of the Electrochemical Society*, **159**, F449 (2012).
5. G. Wu, K. L. More, C. M. Johnston and P. Zelenay, *Science*, **332**, 443 (2011).
6. T. A. Trabold, J. P. Owejan, J. J. Gagliardo, D. L. Jacobson, D. S. Hussey and M. Arif, in *Handbook of Fuel Cells – Fundamentals, Technology and Applications*, W. Vielstich, H. Yokokawa and H. A. Gasteiger Editors, John Wiley & Sons, Ltd, West Sussex, UK (2009).
7. D. S. Hussey and D. L. Jacobson, in *Polymer Electrolyte Membrane and Direct Methanol Fuel Cell Technology*, C. Hartnig and C. Roth Editors, Woodhead Publishing Limited, Cambridge, UK (2011).
8. O. H. W. Siegmund, J. V. Vallerga, A. Martin, B. Feller, M. Arif, D. S. Hussey and D. L. Jacobson, *Nuclear Instruments & Methods in Physics Research Section a-Accelerators Spectrometers Detectors and Associated Equipment*, **579**, 188 (2007).
9. D. S. Hussey, D. L. Jacobson, M. Arif, K. J. Coakley and D. F. Vecchia, *Journal of Fuel Cell Science and Technology*, **7** (2010).
10. J. D. Fairweather, D. Spernjak, A. Z. Weber, D. Harvey, S. Wessel, D. S. Hussey, D. L. Jacobson, K. Artyushkova, R. Mukundan and R. L. Borup, *Journal of The Electrochemical Society*, **160**, F980 (2013).
11. R. Mukundan, D. Spernjak, R. Lujan, J. Fairweather, D. Hussey, D. Jacobson, A. Steinbach, A. Weber and R. L. Borup Neutron imaging and performance of PEMfuel cells with nanostructured thin filmelectrodes at low temperatures, in *224th ECS*, p. 21118, The Electrochemical Society, San Francisco, CA (2013).
12. D. Liu, D. Hussey, M. V. Gubarev, B. D. Ramsey, D. Jacobson, M. Arif, D. E. Moncton and B. Khaykovich *Applied Physics Letters*, **102**, 183508 (2013).